A Class of 2,4-Bisanilinopyrimidine Aurora A Inhibitors with Unusually High Selectivity against Aurora B†

Ignacio Aliagas-Martin,‡ Dan Burdick,‡ Laura Corson,§ Jennafer Dotson,‡ Jason Drummond,‡ Carter Fields,|| Oscar W. Huang,⊥ Thomas Hunsaker,§ Tracy Kleinheinz,‡ Elaine Krueger,‡ Jun Liang,‡ John Moffat,‡ Gail Phillips,|| Rebecca Pulk,‡ Thomas E. Rawson,‡ Mark Ultsch,⊥ Leslie Walker,‡ Christian Wiesmann,⊥ Birong Zhang,‡ Bing-Yan Zhu,‡ and Andrea G. Cochran*,⊥

Departments of Small Molecule Drug Discovery, Cell Regulation, Translational Oncology, and Protein Engineering, Genentech, Inc., 1 DNA Way, South San Francisco, California 94080

Received January 12, 2009

The two major Aurora kinases carry out critical functions at distinct mitotic stages. Selective inhibitors of these kinases, as well as pan-Aurora inhibitors, show antitumor efficacy and are now under clinical investigation. However, the ATP-binding sites of Aurora A and Aurora B are virtually identical, and the structural basis for selective inhibition has therefore not been clear. We report here a class of bisanilinopyrimidine Aurora A inhibitors with excellent selectivity for Aurora A over Aurora B, both in enzymatic assays and in cellular phenotypic assays. Crystal structures of two of the inhibitors in complex with Aurora A implicate a single amino acid difference in Aurora B as responsible for poor inhibitory activity against this enzyme. Mutation of this residue in Aurora B (E161T) or Aurora A (T217E) is sufficient to swap the inhibition profile, suggesting that this difference might be exploited more generally to achieve high selectivity for Aurora A.

Introduction

Aurora kinases are required for mitosis and to complete cell division. Because of this, Aurora kinase inhibitors have been extensively investigated as potential anticancer therapeutic agents. The two major Aurora kinases, Aurora A and Aurora B, are very closely related in kinase domain sequence (71% identical), and the residues lining the binding pocket for the ATP adenine ring are identical. However, the Aurora kinases have quite different, nonoverlapping functions during mitosis.[1,2] This raises the questions of what the preferred inhibition profile might be, Aurora A-selective, Aurora B-selective, or a pan-Aurora inhibitor,[3−6] and how the desired selectivity might be achieved.

The first reported Aurora small-molecule inhibitors appeared to target predominantly Aurora B, despite showing potency against both Aurora kinases in enzymatic assays.[7−9] Aurora B plays sequential roles during mitosis.[1,2] In early mitosis, Aurora B is important for chromosome condensation, a process associated with Aurora B phosphorylation of histone H3 on Ser10. A second major function of Aurora B is to establish correct biorientation and kinetochore attachment of replicated chromosomes and, as part of the spindle assembly checkpoint machinery, to signal an anaphase delay when these conditions are not met. Finally, during late mitosis, Aurora B is necessary for the successful completion of cell division (cytokinesis). Because many Aurora kinase inhibitors cause a characteristic loss of phosphohistone H3, a failure of mitotic arrest in response to taxanes, and cytokinesis failure leading to multinucleated (polyploid) cells, it has been proposed that the mechanism of antitumor efficacy is inhibition of Aurora B.[3] In a more recent example, in vivo efficacy coupled with very high biochemical selectivity for Aurora B has been achieved, providing further justification for this view.[10] Finally, a recent study has demonstrated that mutations in Aurora B selected when cells are exposed to sublethal concentrations of an Aurora B inhibitor are sufficient to confer resistance also to a pan-Aurora inhibitor.[11]

Despite this, significant rationale exists for targeting Aurora A. Aurora A function is evident during early mitosis,[1,2] when it is required for maturation of replicated centrosomes and for maintaining centrosome separation as the bipolar spindle forms. This latter process also requires the mitotic kinesin spindle protein (KSP,[a] also known as HsEg5), a direct substrate of Aurora A. Overexpression of Aurora A has been reported to be transforming in some[12,13] (but not all[12,14]) cell types, and high level expression of Aurora A,[2,4,15] or amplification of the chromosomal region encoding Aurora A,[12,16] has been found in a wide variety of tumors. Of more practical significance, inhibitors of KSP (recently reviewed[5]) and a relatively selective Aurora A inhibitor MLN8054 (**1**, Chart 1)[17] have shown efficacy in tumor models and have entered human clinical trials. Finally, inhibition of Aurora B produces unstable, polyploid cells, some of which potentially remain viable; if this is the case, it is a reason to prefer an Aurora A-selective inhibitor.

One consideration in developing an inhibitor profile is how the agent might combine with other chemotherapeutic drugs. This issue is particularly complex in the case of the Aurora kinases. A number of microtubule-directed drugs induce mitotic arrest by activaton of the spindle assembly checkpoint (SAC), and a sustained[18,19] (but eventually overcome[20]) mitotic arrest

† Coordinates and structure factors have been deposited in the RCSB Protein Data Bank (access codes 3H0Y, 3H0Z, 3H10 for complexes of Aurora A with **5**, **9**, and **15**, respectively).

* To whom correspondence should be addressed. Phone: 650-225-5943. Fax: 650-225-3734. E-mail: andrea@gene.com.

‡ Department of Small Molecule Drug Discovery.

§ Department of Cell Regulation.

|| Department of Translational Oncology.

⊥ Department of Protein Engineering.

[a] Abbreviations: BME, β-mercaptoethanol; CDK, cyclin-dependent kinase; GST, glutathione *S*-transferase; IPTG, isopropyl-β-D-1-thiogalactopyranoside; KSP, kinesin spindle protein; PKI, protein kinase inhibitor; SAC, spindle assembly checkpoint; TEV, tobacco etch virus.

10.1021/jm9000314 CCC: $40.75
Published on Web 04/29/2009

Chart 1. Structure of the Aurora A-Selective[a] Inhibitor **1** (MLN8054)[17]

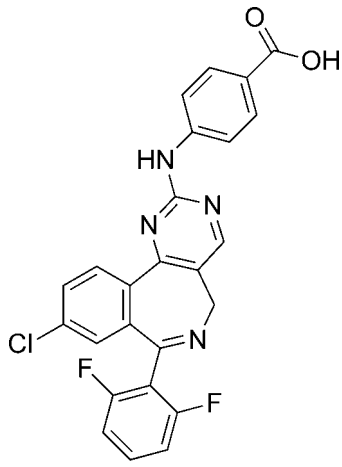

[a] 43-fold selective for Aurora A over Aurora B in enzymatic assays.[17]

is required to trigger eventual apoptosis. Furthermore, it has been reported that a functioning SAC is required in p53-null tumor cells for induction of cell death in response to DNA-damaging agents.[21] Given the importance of Aurora B to SAC function, it might be expected that inhibition of Aurora B would interfere with the action of a number of chemotherapeutic agents. In support of this idea, treatment of cells with the Aurora B inhibitor *N*-[4-[[6-methoxy-7-[3-(4-morpholinyl)propoxy]-4-quinazolinyl]amino]phenyl]benzamide (ZM447439) overrides paclitaxel-induced mitotic arrest.[7]

A second factor influencing drug sensitivity may be variations in the level of Aurora A protein. It has been reported that Aurora A overexpression disrupts SAC function, as indicated by a failure of cells to arrest in response to nocodozole[22] or by premature anaphase entry in the presence of improperly aligned chromosomes and an activated SAC.[14] Furthermore, a reduced sensitivity of HeLa cells overexpressing Aurora A to paclitaxel-induced apoptosis has been noted,[14] while enhanced sensitivity to paclitaxel and docetaxel has been reported for pancreatic cancer cell lines in which Aurora A was knocked down by siRNA.[23]

Taken together, these data strongly suggest that conflicting effects might occur when both Aurora kinases are inhibited pharmacologically and that the net outcome in combination with other drugs may be difficult to predict. Therefore, in order to rationally approach this problem, it will be important to test drug combinations using inhibitors with clean Aurora A or Aurora B inhibition profiles. Compound **1** is potentially a useful Aurora A-selective agent for this purpose; however, in cellular assays, there is only a narrow concentration range (<8-fold) over which **1** fully inhibits Aurora A and does not detectably inhibit Aurora B.[17] We describe here a new series of dianilinopyrimidines showing very high selectivity for Aurora A in cellular assays.

Chemical Synthesis

Focused libraries of 2,4-diamino-5-fluoropyrimidine derivatives were prepared in a straightforward fashion via 2,4-dichloro-5-fluoropyrimidine (Scheme 1). Briefly, the chlorine atoms of 5-fluoro-2,4-dichloropyrimidine derivative **2** were sequentially displaced with the appropriate nucleophiles to yield the desired 2,4-dianilinopyrimidines. For example, reflux of **2** and commercially available *N*-(4-aminophenyl)-2-chlorobenzamide **3** in ethanol yielded the monosubstituted intermediate **4**. Subsequent microwave irradiation of **4** and 4-aminophenol gave the bis-anilinopyrimidine **5**. Alternatively, for 2-(4-aminophenylacetic acid amide)-substituted pyrimidines such as **9** and **10**, the initial chloro displacement by 4-amino-*N*-(2-chlorophenyl)benzamide **6** (yielding *o*-chloroaniline intermediate **7**) was followed by displacement of the second chlorine atom by 4-aminophenylacetic acid. The desired amide analogues were then prepared in standard fashion.

Results and Discussion

In an effort to identify lead inhibitors, we undertook a screening campaign against Aurora A kinase and identified two symmetrically substituted 5-fluoro-2,4-bisanilinopyrimidines of submicromolar IC_{50} (Chart 2). Disubstituted aminopyrimidines are a versatile class of kinase inhibitors. Both 2,4- and 4,6-bisanilinopyrimidines have been explored as cyclin-dependent kinase (CDK) inhibitors, with reported examples showing selectivity for CDK4 over CDK2[24,25] or the reverse.[26] These[27,28] and related[29] structural scaffolds have also yielded potent Aurora A inhibitors. One strength of the bisanilinopyrimidine scaffold is that it is readily adaptable to combinatorial synthesis.[28]

To explore the requirements for high-affinity binding to Aurora A, we prepared a series of focused libraries (Supporting Information Tables S1−S6). From a series in which the A and B rings (Chart 2) were identical, we determined that the *p*-hydroxyaniline analogue had improved affinity ($IC_{50} = 0.03$ μM; **18**, Table S1). We then established that substitutions at position 6 of the pyrimidine completely abolished binding. At the 5 position of the pyrimidine ring, smaller aliphatic groups were tolerated, while electron-withdrawing substituents, especially halogens, were prefererred (Table S2). A library including regioisomers of methyl- and methoxy-substituted anilines at the B ring revealed that, in both cases, *o*- and *p*-substitution increased potency relative to the *m*-substituted analogues (2- to 10-fold, Table S3). In a recent crystallographic study, the binding mode to Aurora A of a 2,4-bisanilinopyrimidine bearing *m*-substituted anilines was characterized, but the preferred regioisomers were not determined.[27]

At this stage we decided to further explore substitution of the B-ring through a library of *p*-aminobenzoic acid amides (Chart 3). This effort revealed a preference for primary amides with larger hydrophobic substitutions, especially aryl (Table S4). Within the arylamide series, a fairly uniform potency was observed (~0.02−0.08 μM), with the exception of *o*-fluoro and *o*-chloro analogues, which were somewhat more potent (0.009 and 0.010 μM, respectively; Table S5). Reversal of the amide orientation as, for example, in compound **5** did not greatly affect potency (Tables 1 and S6).

Our preliminary exploration of the pyrimidine scaffold demonstrated that it was possible to find many inhibitors having significant affinity for Aurora A and several with $IC_{50} < 10$ nM. This is not especially surprising, given the general utility of this scaffold and the large variety of structurally diverse scaffolds that yield potent inhibitors of Aurora A. However, we were surprised to find that many of the more potent compounds from the library depicted in Chart 3 were also selective for Aurora A. For example, the *o*-chlorophenylamide **13** is 190-fold more potent against Aurora A than against Aurora B (Chart 4). Further testing against a panel of 30 kinases revealed generally good selectivity (Supporting Information Table S7).

Although these compounds were potent inhibitors of the Aurora A enzyme, their antiproliferative activity was not correspondingly high (Chart 4). We therefore modified the A

Scheme 1. Synthesis of 2,4-Bisanilinopyrimidines[a]

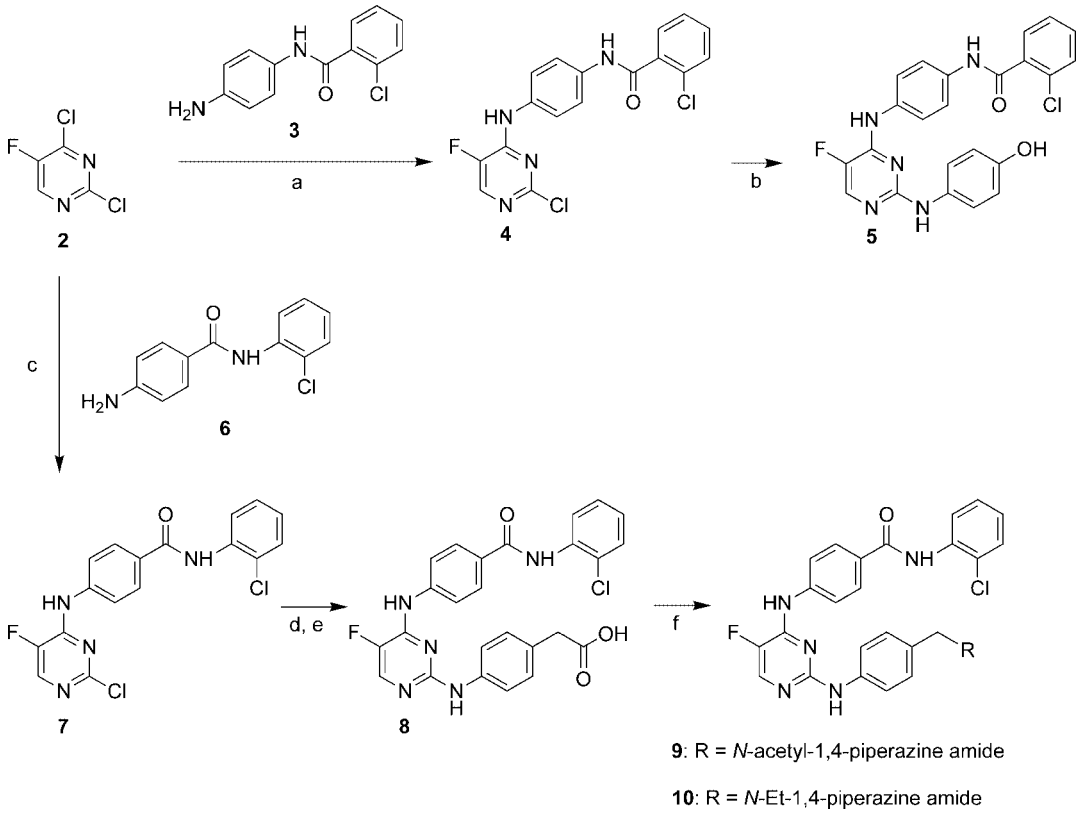

[a] (a) DIPEA, EtOH, reflux; (b) 4-aminophenol, HCl, *n*-BuOH, 150 °C; (c) DIPEA, MeOH, 70 °C; (d) 4-aminophenylacetic acid, EtOH, 180 °C; (e) $LiOH/H_2O$; (f) substituted piperazine, HOBT/EDC (**9**) or TBTU (**10**), DIPEA, DMF.

Chart 2. 2,4-Bisanilinopyrimidine Inhibitors of Aurora A Discovered in a High-Throughput Screen

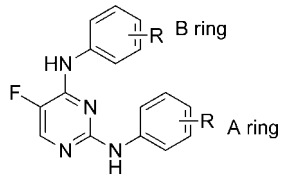

11: R = *m*-Me; IC_{50} = 0.68 μM
12: R = *p*-OMe; IC_{50} = 0.13 μM

Chart 3. B Ring Benzoic Acid Amide Library

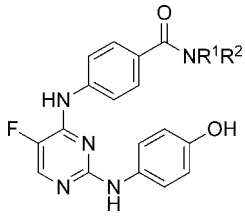

ring with groups designed to improve solubility and/or permeability, yielding, for example, the exceptionally Aurora A-selective **9** and **10** (Scheme 1, Table 1, Supporting Information Table S8). Despite making scores of analogues of this type (not shown), we were largely unsuccessful in improving the antiproliferative IC_{50} values, which remained in the vicinity of 1 μM (HCT116). More importantly, the narrow range of cellular activities offered little opportunity to propose (or test) structure−activity relationships. To determine whether the observed antiproliferative activities of our inhibitors nevertheless reflected intracellular inhibition of Aurora A, we evaluated their

Table 1. In Vitro Activities of 2,4-Bisanilinopyrimidines and **1**[a]

	IC_{50}, μM					
compd	Aurora A	Aurora B	B/A ratio	CDK2/cyclinA	HCT116	HT29
1	0.0010	0.0093	9.3	nd[b]	0.10	0.15
5	0.0060	1.4	230	nd[b]	0.85	7.2
13	0.010	1.9	190	3.2	0.87	17
14	0.054	3.8	70	nd[b]	2.0	27
9	0.0043	3.7	860	>16	0.64	6.2
10	0.0034	3.4	1000	>16	0.19	2.9

[a] Values for **1** determined in our assays for comparison purposes. [b] Not determined.

potency in phenotypic immunofluorescence assays[30] (Table 2). We could detect inhibition of Aurora A, as indicated by a failure of centrosome separation and loss of phospho-Aurora A immunostaining at the centrosomes. In contrast, no loss of phosphohistone H3 immunostaining was apparent at the concentrations tested, indicating that, as expected, these compounds do not inhibit Aurora B. The concentrations necessary to inhibit Aurora A function in HCT116 cells are close to those needed to block proliferation, suggesting that these effects are correlated. However, off-target contributions to the antiproliferative activity cannot be ruled out.

We determined enzymatic IC_{50} values for several analogues against different forms of the Aurora A enzyme, including a complex with a peptide from the intracellular activator TPX2[31] (Table 3). We see no loss of potency against the full-length wild-type enzyme when compared to the mutant kinase domain used for routine screening; IC_{50} values for the two enzyme forms were all within ~3-fold. Importantly, inhibition of the TPX2 peptide complex (arguably the form most relevant to intracellular Aurora A) was very similar to inhibition of the free full-length enzyme (within 2-fold). These data suggest that the generally

Chart 4. Aurora A-Selective 2,4-Bisanilinopyrimidines[a]

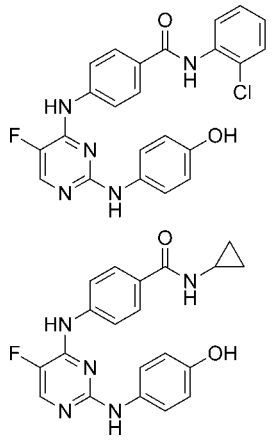

13:

	IC_{50}, μM
AurA	0.010
AurB	1.9
HCT116	0.88
HT29	17

14:

	IC_{50}, μM
AurA	0.054
AurB	3.8
HCT116	2.0
HT29	27

[a] IC_{50} values are for enzymatic and cellular proliferation assays as described in the Experimental Section.

lower potency in cellular assays compared to enzymatic assays might reflect a problem with the physical properties of this lead series (resulting in relatively low intracellular concentrations of inhibitor). An additional possibility is that a very high fractional inhibition of Aurora A may be required to block proliferation and Aurora A functional readouts.[32]

One noteworthy trend in the cellular assays was the lesser antiproliferative activity for many compounds against the colon cancer cell line HT29 compared to that against HCT116 (for example, see Table 1). We retested several compounds in HT29 cells using the phospho-Aurora A immunofluorescence assay described above and found little or no difference in Aurora A inhibition in the two cell lines (not shown). This suggests that HT29 cells may be more resistant to the antiproliferative effects of Aurora A inhibition. This difference in sensitivity has been noted previously for an inhibitor of the mitotic kinesin KSP, a direct substrate of Aurora A, and it has been attributed to a failure of HT29 cells to bypass the spindle checkpoint after its sustained activation (mitotic slippage).[33] It may, therefore, be a property characteristic of Aurora A pathway inhibition. A more recent study demonstrates that mitotic cell death of HT29 cells treated with KSP inhibitors is dramatically reduced if inhibition is less than fully penetrant.[34] This situation appears not to apply here, as we can observe apparently complete inhibition of Aurora A in HT29.

To understand better the structural basis for selective Aurora A inhibition, we determined the cocrystal structures of **5** and **9** bound to Aurora A (2.5 and 2.9 Å resolution, respectively). The pyrimidine binding mode is in both cases fully consistent with reported structures of similar ligands bound to Aurora A[27] or to CDK2.[24] The 2,4-bisanilinopyrimidine core forms the expected hydrogen bonds to the hinge region of the kinase and adopts a horseshoe-shaped, *s*-cis conformation (Figure 1A). This directs the B ring amide substituent back toward solvent and past the pocket normally occupied by the ATP ribose ring. One difference seen between the present structures and a recently published Aurora A pyrimidine complex structure (PDB code 2NP8[27]) is that the B rings here are tilted considerably out of the plane of the pyrimidine ring (Figure 1A). Similar deviations have been noted in structures of bisanilinopyrimidines in complex with CDK2.[24]

The ATP binding pockets of Aurora A and Aurora B are virtually identical in composition. Those differences that do exist are near the exterior of the pocket (Figure 1B). Only one of these amino acid side chains, Thr217, appears to be in direct contact with bound ADP (not shown, PDB code 1MQ4[36]), through the 2′-hydroxyl group of the ribose ring. The large amide substituents of inhibitors **5** and **9** extend to the outer portion of the binding pocket through a region adjacent to Thr217. The binding pocket narrows near Thr217 (Figure 1C), suggesting that the larger residue present in Aurora B (Glu161) would block access to the outer portion of the binding pocket. Therefore, of the three residues that differ between Aurora A and Aurora B, Thr 217 appeared most likely to govern specificity for inhibitor binding.

We tested this idea by making single amino acid substitutions in Aurora A (T217E) and Aurora B (E161T). Mutant kinases were expressed and purified as described for full-length Flag-tagged Aurora A and were found to have very similar activities as their wild-type counterparts (not shown). Inhibitors **9** and **10** were tested against each wild-type kinase and the two mutants (Figure 2, Table 4). The inhibitory potencies of **9** and **10** were strongly affected by the single amino acid substitutions. For either Aurora kinase, the presence of threonine allowed potent inhibition, while for glutamic acid variants, there was a substantial shift in IC_{50} (approximately 100-fold). This supports a "gating" role for this residue; presumably, the Aurora B binding pocket is enlarged by the E161T mutation, while the pocket is closed in Aurora A by the T217E mutation. As might be expected, IC_{50} values for the pan-Aurora inhibitor *N*-[4-[[4-(4-methyl-1-piperazinyl)-6-[(5-methyl-1*H*-pyrazol-3-yl)amino]-2-pyrimidinyl]thio]phenyl]cyclopropanecarboxamide (VX-680)[9] varied no more than 2-fold against either kinase and its mutant form (not shown).

Compound **1** is a recently described inhibitor that shows 43-fold selectivity for Aurora A over Aurora B in enzymatic assays.[17] Selectivity for Aurora A can be seen in cell-based assays, and the inhibitor has shown antitumor efficacy in mouse xenograft models.[17] To assess whether the selectivity of **1** might be explained by a similar steric conflict with the Glu161 side chain of Aurora B, we determined the 2.2 Å cocrystal structure of the closely related compound **15** bound to Aurora A (Figure 3). The 2,5-difluorophenyl group occupies a space near that occupied by the *o*-chlorophenyl groups of **5** and **9**. This suggests that the 2,5-difluorophenyl substituent may be driving selectivity in a similar manner; however, this group does not approach as closely to Thr217. This observation is consistent with the idea that Thr217 is the critical difference between Aurora A and Aurora B and with the enhanced selectivity we observe for inhibitors **9** and **10** compared to that reported for **1**.[17] The Thr217/Glu161 difference has been proposed recently to explain the selectivity of indirubin-based inhibitors for Aurora B.[37] In this case, molecular modeling suggested that Glu161 contributes a hydrogen bond interaction with bound ligand that is not achievable by the shorter Thr217 side chain in Aurora A.

Conclusions

We establish here a structural basis for very high selectivity in a class of 2,4-dianilinopyrimidine inhibitors of Aurora A. A relatively small amino acid side chain, that of Thr217, accommodates inhibitor binding, while the larger side chain present in Aurora B, that of Glu161, does not. Interestingly, the equivalent residue in human kinases is commonly aspartic acid or glutamic acid (∼50%), while threonine is relatively rare (∼6%). Small residues (Thr, Ser, Ala) together account for ∼35%.[38] For mammalian Aurora B and Aurora C, it is always glutamic acid, while Aurora A sequences invariably have

Table 2. Thresholds for Complete Cellular Inhibition of Aurora A or Aurora B[a]

compd	centrosome separation, HCT116	pT288-AurA, HCT116	p-S10-histone H3[b]		proliferation IC_{50}, HCT116
			HCT116	HT29	
1	0.16	0.31	5.0	nd[c]	0.10
5	1.6	nd[c]	>12	>30	0.85
13	1.6	5.0	>25	>30	0.87
14	6.3	nd[c]	>25	>30	2.0
9	1.6	2.5	>25	>27	0.64
10	0.39	2.5	>50	>27	0.19

[a] Immunofluorescence assays were conducted as previously described,[30] and data are reported as the lowest inhibitor concentration at which visual scoring indicated *complete* inhibition. (Therefore, the reported value is higher than IC_{50}.) All values are reported in μM. [b] No loss of p-H3 (even partial) was evident at the highest tested concentrations of pyrimidine inhibitors (those listed in the table). [c] Not determined.

Table 3. Relative IC_{50} Values for Aurora A Inhibitors Tested against Different Forms of the Enzyme[a]

compd	kinase domain[b]	full-length Aurora A[c]	TPX2 complex[d]
5	1	0.40	0.65
13	1	0.31	0.27
14	1	0.35	0.40
9	1	0.32	0.32
10	1	0.36	0.19

[a] Inhibition data for each compound are normalized to the value determined for inhibition of the kinase domain. Enzyme reactions were conducted identically at 30 μM ATP and 5 nM enzyme for kinase domain and full-length forms or 2 nM enzyme for the TPX2 complex. [b] The kinase domain construct has been described previously.[30] [c] Full-length wild-type Aurora A with an amino-terminal Flag tag (see Experimental Section). [d] Full-length wild-type Aurora A coexpresssed with a glutathione *S*-transferase (GST) fusion of TPX2 2−43 (see Experimental Section).

threonine or alanine at this position. It is tempting therefore to ask whether this difference might be functionally important. The crystal structure of protein kinase A in complex with the pseudosubstrate protein kinase inhibitor (PKI, PDB code 1ATP[39]) shows the equivalent residue (Glu) engaging in a salt bridge with an arginine residue at the −3 position of PKI. Aurora kinases also phosphorylate basic substrates, so the change from glutamic acid to threonine may influence substrate sequence preference.

Inhibitors **9** and **10** are exceptionally selective Aurora A inhibitors; we can see no indications in cellular assays that they inhibit Aurora B or CDKs. As such, they are useful tool compounds for investigating the cellular role of Aurora A kinases without the complication of also inhibiting Aurora B.

Experimental Section

Enzymatic and Cellular Assays. Aurora A and Aurora B IC_{50} determinations were conducted as described previously using a histone H3 peptide as substrate.[30] Antiproliferative and phenotypic immunofluorescence assays were also as described.[30]

Crystallography. Aurora A inhibitor complexes were cocrystallized as described previously[30] except that the proteins used were K124A, T287A, T288A. Structures were solved by molecular replacement as previously described.[30]

Full-Length Wild-Type and Mutant Kinases. The E161T Aurora B and T217E Aurora A variants were prepared from wild-type, full-length, N-terminally Flag-tagged (Sigma) coding sequences cloned into pET-21a (EMD Biosciences) by standard Kunkel mutagenesis. All constructs were sequence verified. Mutants and the corresponding wild-type control proteins were expressed in *E. coli* BL21-DE3 pLysS-Rosetta (EMD Biosciences) and purified as previously described.[30]

The complex of TPX2 and Aurora A was prepared by cloning of a GST fusion of TPX2 residues 2−43 behind a second T7-lac promoter into the pET21 Aurora A construct described above. The linker between GST and the TPX2 sequence included a tobacco etch virus (TEV) protease site. The complex was expressed in *E. coli* BL21-DE3 pLysS-Rosetta 2 (EMD Biosciences) at 37 °C by induction with 1 mM isopropyl-β-D-1-thiogalactopyranoside (IPTG). Cells were harvested after 3 h. Cell lysates were prepared by suspension in 50 mM Tris, pH 8, 0.4 M NaCl, 1 mM EDTA, 5 mM β-mercaptoethanol (BME), 5% glycerol (buffer A) and passage

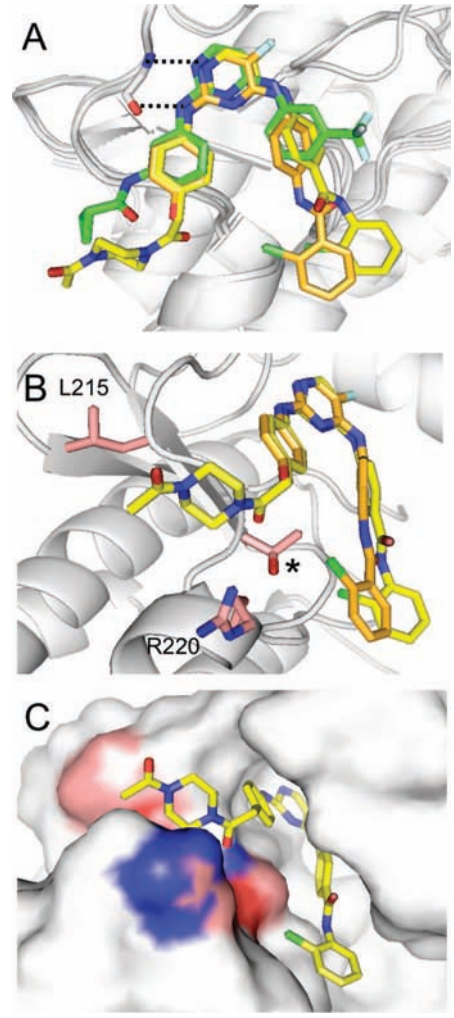

Figure 1. Cocrystal structures of Aurora A and Aurora A-selective inhibitors. (A) Overlaid complex structures of **5** (orange) and **9** (yellow) with a published example of a bisanilinopyrimidine (green) bound to Aurora A (PDB code 2NP8[27]). In each case, Aurora A is depicted in white ribbon. Hydrogen bonds to the kinase hinge region are indicated by dotted lines. In parts A and B, all amino terminal residues up to 151 (including the phosphate-binding loop) are left out of the representation to help better visualize ligands. (B) Residues of Aurora A in the vicinity of the binding pocket that differ in Aurora B. Leu215, Thr217, and Arg220 side chains are shown in pink. In Aurora B, the equivalent residues are Arg159, Glu161, and Lys164, respectively. Of these, Thr217 (marked by asterisk) is in closest proximity to bound ligands. (C) Surface representation of Aurora A bound to **9**. The orientation and residue coloring are the same as those shown in B. All images shown here were prepared using Pymol.[35]

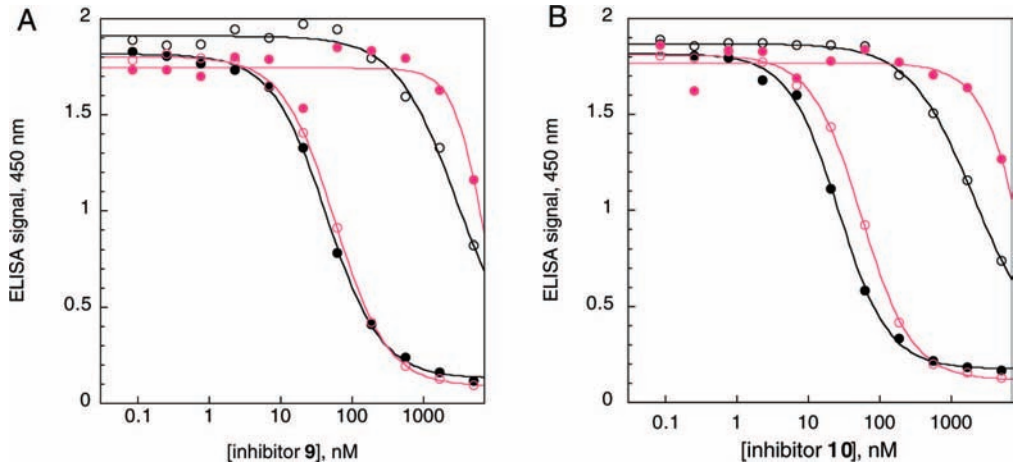

Figure 2. Switching the ligand-binding specificity of Aurora A and Aurora B for (A) inhibitor **9** or (B) inhibitor **10**. IC_{50} curves were determined for inhibition of wild-type enzymes (solid symbols; Aurora A, black; Aurora B, pink), T217E Aurora A (open symbols, black), and E161T Aurora B (open symbols, pink). In all cases, [ATP] = 30 μM ($\sim K_m$). Aurora A enzyme concentration was 5 nM, while Aurora B enzymes were used at 75 nM. Note that these enzyme concentrations are higher than those of the optimized screening assay[30] used to generate the SAR tables and that IC_{50} values fitted to these data (Table 4) are accordingly somewhat higher. For all enzymes, signal was determined to be linear with enzyme concentration at the concentration used (not shown).

Table 4. Inhibition of Aurora A and Aurora B Mutants[a]

	IC_{50}, μM	
	compound **9**	compound **10**
Aurora A wild-type	0.044	0.026
Aurora A T217E	2.8	2.0
Aurora B wild-type	6.8	~20
Aurora B E161T	0.057	0.055

[a] IC_{50} values for the experiments shown in Figure 2. See figure caption for experimental details.

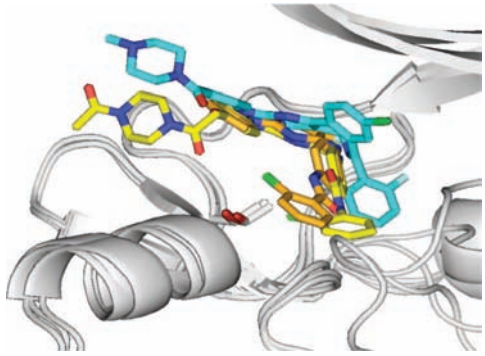

Figure 3. Structures of the complexes of **5** (orange) and **9** (yellow) overlaid on the structure of Aurora A bound to the *N*-Me-1,4-piperazineamide derivative of **1** (compound **15**, cyan). The Thr217 side chains are represented as sticks. Amino terminal residues of Aurora A are omitted as in Figure 1. The image shown here was prepared using Pymol.[35]

through a microfluidizer. The soluble fraction was loaded onto glutathione Sepharose 4B (Amersham Biosciences), and the column was washed with buffer A. Aurora A complex and excess GST-TPX2 were eluted with 10 mM glutathione in buffer A. Protein was loaded onto anti-Flag M2 agarose (Sigma) equilibrated in 20 mM HEPES, pH 7.2, 0.4 M NaCl, 5 mM BME, 20% glycerol (buffer B). After being washed, the complex was eluted with 100 μg/mL Flag peptide (Sigma) in buffer B. Final purification was achieved by passage through a HiLoad Superdex 16/60 S-200 column equilibrated in buffer B. Note that we eventually chose not to cleave the TPX2 peptide from the GST fusion partner. We observed that the TPX2 fragment stained quite poorly on gels, and we could not be certain that it was still present in the complex at stoichiometric levels after TEV protease cleavage.

General Synthetic Procedures. Reagents were purchased at the highest commercial quality available and were used without further purification. E. Merck silica gel (60, particle size 0.040−0.063 mm) was used for flash column chromatography. NMR spectra were recorded on Varian 400 instruments and were calibrated using chemical shifts of residual undeuterated solvent. The following abbreviations were used to explain the multiplicities: s = singlet, d = doublet, t = triplet, q = quartet, m = multiplet, dd = doublet of doublet. Electrospray ionization (ESI) mass spectrometry (MS) experiments were performed on an API100 Perkin-Elmer SCIEX single quadrupole mass spectrometer at 4000 V emitter voltage. Yields refer to chromatographically and spectroscopically (^{1}H NMR) homogeneous materials, unless otherwise stated. Purities of assayed compounds were in all cases greater than 95%, as determined by reversed-phase HPLC analysis.

2-Chloro-*N*-(4-(2-chloro-5-fluoropyrimidin-4-ylamino)phenyl)-benzamide (4). A solution of commercially available *N*-(4-aminophenyl)-2-chlorobenzamide (**3**, 100 mg, 0.40 mmol), 2,4-dichloro-5-fluoropyrimidine (**2**, 70 mg, 0.40 mmol), and 100 μL of DIPEA (1.0 mmol) in 5 mL of ethanol was heated at reflux for 6 h. The solvent was evaporated and the residue partitioned between water and DCM. The DCM phase was concentrated, and the crude product was purified on silica gel (98/2 DCM/MeOH) to give **4** (110 mg, 70%). MS (ESI+) m/z = 377.2 (M + 1, 2 Cl isotope pattern); ^{1}H NMR (400 MHz, $CDCl_3$) δ 8.06 (d, J = 2.7 Hz, 1H), 7.95 (s, 1H), 7.82−7.73 (m, 1H), 7.66 (q, J = 9.0 Hz, 4H), 7.50−7.33 (m, 3H), 7.02 (s, 1H).

2-Chloro-*N*-(4-(5-fluoro-2-(4-hydroxyphenylamino)pyrimidin-4-ylamino)phenyl)benzamide (5). A mixture of **4** (49 mg, 0.13 mmol), 4-aminophenol (28 mg, 0.26 mmol), 2.5 mL butanol, and 1 drop of 37% HCl was heated by microwave in a sealed tube at 150 °C for 30 min. Solvents were evaporated and the residue purified by HPLC (C18, 0−60 acetonitrile in water, 0.1% TFA). Fractions were combined and lyophilized to give **5** (45.2 mg, 77%). MS (ESI+) m/z = 450.2 (M + 1, 1 Cl isotope pattern); ^{1}H NMR (400 MHz, DMSO-d_6) δ 10.49 (s, 1H), 9.98−9.84 (m, 1H), 9.47−9.36 (m, 1H), 9.36−9.09 (m, 1H), 8.08 (d, J = 4.5 Hz, 1H), 7.71 (dd, J = 9.0, 24.0 Hz, 4H), 7.57 (d, J = 7.5 Hz, 2H), 7.54−7.41 (m, 2H), 7.31 (d, J = 8.8 Hz, 2H), 6.72 (d, J = 8.8 Hz, 2H); HRMS m/z = 450.1135 (M + H), calcd ($C_{23}H_{17}ClFN_5O_2$ + H) = 450.1133.

4-(2-Chloro-5-fluoropyrimidin-4-ylamino)-*N*-(2-chlorophenyl)-benzamide (7). A mixture of 2,4-dichloro-5-fluoropyrimidine (**2**, 7.84 g, 46.9 mmol), commercially available 4-amino-*N*-(2-chlorophenyl)benzamide (**6**, 3.84 g, 15.6 mmol), DIPEA (1.5 mL, 15.6 mmol), and 100 mL of methanol was heated to 70 °C for 72 h.

The reaction mixture was cooled and the yellow crystalline product collected by filtration to give **7** (5.068 g, 89%), which was used without further purification. MS (ESI+) $m/z = 377.0$ (M + 1) 2 Cl isotope pattern; ^{1}H NMR (500 MHz, DMSO-d_6) δ 10.28 (s, 1H), 9.98 (s, 1H), 8.42 (d, $J = 3.3$ Hz, 1H), 8.02 (d, $J = 8.7$ Hz, 2H), 7.89 (d, $J = 8.7$ Hz, 2H), 7.62 (d, $J = 6.9$ Hz, 1H), 7.57 (d, $J = 7.1$ Hz, 1H), 7.40 (t, $J = 7.2$ Hz, 1H), 7.30 (dd, $J = 4.4$, 11.0 Hz, 1H).

2-(4-(4-(4-(2-Chlorophenylcarbamoyl)phenylamino)-5-fluoropyrimidin-2-ylamino)phenyl)acetic Acid (8). A sealed microwave vial containing a mixture of **7** (539 mg, 1.43 mmol), commercially available 2-(4-aminophenyl)acetic acid (642 mg, 4.25 mmol), 3 mL of ethanol, and 1 mL of 37% HCl was heated to 180 °C in a microwave reactor for 10 min. Analysis of the reaction mixture indicated that substitution was complete but with substantial ethyl ester formation. The concentrated reaction mixture was therefore heated to 40 °C in a solution of 10 mL of water and 3 mL of 1 N LiOH for 4 h, by which time hydrolysis was complete. The reaction mixture was concentrated under vacuum and purified by HPLC to yield **8** (575 mg, 82%). MS (ESI+) $m/z = 492.1$ (M + 1); ^{1}H NMR (500 MHz, DMSO-d_6) δ 9.93 (s, 1H), 9.81 (s, 1H), 9.45 (s, 1H), 8.21 (d, $J = 3.7$ Hz, 1H), 8.00 (dd, $J = 8.8$, 20.8 Hz, 4H), 7.69−7.47 (m, 4H), 7.40 (t, $J = 7.7$ Hz, 1H), 7.30 (t, $J = 7.7$ Hz, 1H), 7.17 (d, $J = 8.5$ Hz, 2H), 3.50 (s, 2H).

4-(2-(4-(2-(4-Acetylpiperazin-1-yl)-2-oxoethyl)phenylamino)-5-fluoropyrimidin-4-ylamino)-*N*-(2-chlorophenyl)benzamide (9). A mixture of compound **8** (151 mg, 0.31 mmol), 1-acetylpiperazine (78.1 mg, 0.62 mmol), HOBT (47 mg, 0.338 mmol), EDC (88.2 mg, 0.46 mmol), DIPEA (107 μL, 1.1 mmol), and 3 mL of DMF was stirred at 45 °C overnight. The reaction mixture was concentrated, and the crude product was purified by HPLC to give **9** (35.4 mg, 19%). MS (ESI+) $m/z = 602.2$ (M + 1); ^{1}H NMR (400 MHz, DMSO-d_6) δ 9.87 (s, 1H), 9.74 (s, 1H), 9.35 (s, 1H), 8.19 (d, $J = 3.8$ Hz, 1H), 7.99 (q, $J = 9.0$ Hz, 4H), 7.72−7.48 (m, 4H), 7.40 (t, $J = 7.7$ Hz, 1H), 7.30 (d, $J = 7.8$ Hz, 1H), 7.14 (d, $J = 8.4$ Hz, 2H), 3.68 (s, 3H), 3.35 (s, 4H), 1.96 (d, $J = 7.0$ Hz, 3H); HRMS $m/z = 602.2087$ (M + H), calcd ($C_{31}H_{29}ClFN_7O_3$ + H) = 602.2083.

***N*-(2-Chlorophenyl)-4-(2-(4-(2-(4-ethylpiperazin-1-yl)-2-oxoethyl)phenylamino)-5-fluoropyrimidin-4-ylamino)benzamide (10).** A mixture of **8** (71 mg, 0.14 mmol), 1-ethylpiperazine (18 μL, 0.14 mmol), TBTU (51 mg, 0.16 mmol), DIPEA (55 μL, 0.57 mmol), and 5 mL of DMF was stirred overnight at which point the reaction was judged complete by LC/MS analysis. The mixture was concentrated under vacuum, and the residue was purified by HPLC to give **10** (66.1 mg, 78%). MS (ESI+) $m/z = 588.0$ (M + 1); ^{1}H NMR (400 MHz, DMSO-d_6) δ 9.89 (s, 1H), 9.67 (s, 1H), 9.53−9.36 (m, 1H), 9.30 (s, 1H), 8.18 (d, $J = 3.6$ Hz, 1H), 8.00 (dd, $J = 8.9$, 20.9 Hz, 4H), 7.69−7.48 (m, 4H), 7.39 (d, $J = 7.7$ Hz, 1H), 7.31 (d, $J = 6.2$ Hz, 1H), 7.12 (d, $J = 8.5$ Hz, 2H), 4.52−4.37 (m, 1H), 4.28−4.09 (m, 1H), 3.70 (s, 2H), 3.13 (s, 2H), 2.90 (s, 3H), 1.18 (t, $J = 7.3$ Hz, 3H); HRMS $m/z = 588.2068$ (M + H), calcd ($C_{31}H_{31}ClFN_7O_2$ + H) = 588.2290.

5-Fluoro-N^2,N^4-dim-tolylpyrimidine-2,4-diamine (11). A mixture of 2,4-dichloro-5-fluoropyrimidine (**2**, 150 mg, 0.9 mmol), *m*-toluidine (386 μL, 3.6 mmol), DIPEA (340 μL, 3.5 mmol), and 3 mL of dioxane was heated by microwave in a capped vial at 160 °C for 20 min. The reaction mixture was cooled and concentrated under vacuum to give 668 mg of crude product. Crude product (50 mg) was purified by reversed-phase HPLC (acetonitrile/water/0.1% formic acid) to give **11** (17.2 mg, 83%). MS (ESI+) $m/z = 309.2$ (M + 1); ^{1}H NMR (400 MHz, DMSO-d_6) δ 9.21 (s, 1H), 9.08 (s, 1H), 8.08 (d, $J = 3.8$ Hz, 1H), 7.62−7.52 (m, 2H), 7.45 (d, $J = 8.9$ Hz, 2H), 7.21 (t, $J = 7.8$ Hz, 1H), 7.08 (t, $J = 7.7$ Hz, 1H), 6.90 (d, $J = 7.5$ Hz, 1H), 6.71 (d, $J = 7.5$ Hz, 1H), 2.29 (s, 3H), 2.20 (s, 3H).

5-Fluoro-N^2,N^4-bis(4-methoxyphenyl)pyrimidine-2,4-diamine (12). A mixture of 2,4-dichloro-5-fluoropyrimidine (**2**, 134 mg, 0.8 mmol), 4-methoxyaniline (394 μL, 3.2 mmol), DIPEA (340 μL, 3.5 mmol) in 3 mL of dioxane was heated by microwave in a capped vial at 160 °C for 20 min. The reaction mixture was cooled, and the solvents were removed under vacuum to give 523 mg of crude product. Then 50 mg of the crude product was purified by reversed-phase HPLC (acetonitrile/water/0.1% formic acid) to give **12** (31 mg, 100% calcd as the bis formate salt). MS (ESI+) $m/z = 341.2$ (M + 1); ^{1}H NMR (400 MHz, DMSO-d_6) δ 9.12 (s, 1H), 8.88 (s, 1H), 7.99 (d, $J = 3.8$ Hz, 1H), 7.64 (d, $J = 9.0$ Hz, 2H), 7.52 (d, $J = 9.0$ Hz, 2H), 6.90 (d, $J = 9.0$ Hz, 2H), 6.79 (d, $J = 9.0$ Hz, 2H), 3.76 (s, 3H), 3.71 (s, 3H).

***N*-(2-Chlorophenyl)-4-(5-fluoro-2-(4-hydroxyphenylamino)pyrimidin-4-ylamino)benzamide (13).** Starting from intermediate **7** and using a procedure identical to that used to synthesize compound **5**, compound **13** was produced. MS (ESI+) $m/z = 450.5$ (M + 1, 1 Cl isotope pattern); ^{1}H NMR (400 MHz, DMSO-d_6) δ 9.99 (s, 1H), 9.91 (s, 1H), 9.40 (s, 1H), 9.20 (s, 1H), 8.15 (d, 1H), 7.95 (m, 4H), 7.60 (dd, 1H), 7.54 (dd, 1H), 7.24−7.40 (m, 4H), 6.72 (m, 2H); HRMS $m/z = 450.1135$ (M + H), calcd ($C_{23}H_{17}ClFN_5O_2$ + H) = 450.1133.

***N*-Cyclopropyl-4-(5-fluoro-2-(4-hydroxyphenylamino)pyrimidin-4-ylamino)benzamide (14).** A mixture of 2,4-dichloro-5-fluoropyrimidine (242 mg, 1.45 mmol), commercially available 4-amino-*N*-cyclopropylbenzamide (255 mg, 1.45 mmol), potassium carbonate (200 mg, 1.45 mmol), and 10 mL of DMF was heated to 60 °C overnight. The reaction mixture was partitioned between ethyl acetate and saturated ammonium chloride, and the organic layer was concentrated. The crude product was purified by flash chromatography on silica gel (ethyl acetate/hexanes) to give 4-(2-chloro-5-fluoropyrimidin-4-ylamino)-*N*-cyclopropylbenzamide (76 mg, 17%). MS (ESI+) $m/z = 307.2$ (M + 1); ^{1}H NMR (400 MHz, DMSO-d_6) δ 10.15 (s, 1H), 8.35 (dd, $J = 3.7$, 18.2 Hz, 2H), 7.86−7.69 (m, 5H), 2.90−2.76 (m, 1H), 0.73−0.62 (m, 3H), 0.60−0.45 (m, 3H). A capped microwave vial containing the benzamide product (70 mg, 0.2 mmol), 4-aminophenol (50 mg, 0.4 mmol), 4 M HCl in dioxane (0.11 mL, 0.4 mmol), and 2.5 mL of butanol was heated by microwave at 150 °C for 30 min. Solvents were removed under vacuum, and the crude product was purified by flash chromatography on silica gel (ethyl acetate/hexanes) to give **14** (14.4 mg, 20%). MS (ESI+) $m/z = 380.2$ (M + 1); ^{1}H NMR (400 MHz, DMSO-d_6) δ 9.45 (s, 1H), 9.08 (s, 1H), 8.95 (s, 1H), 8.31 (d, 1H), 8.09 (d, 1H), 7.90 (d, 2H), 7.77 (d, 2H), 7.36 (d, 2H), 6.69 (d, 2H), 2.81 (m, 1H), 0.7 (m, 2H), 0.57 (m, 2H); HRMS $m/z = 380.1608$ (M + H), calcd ($C_{20}H_{18}FN_5O_2$ + H) = 380.1523.

Acknowledgment. Portions of this research were carried out at the Stanford Synchrotron Radiation Laboratory, a national user facility operated by Stanford University on behalf of the U.S. Department of Energy, Office of Basic Energy Sciences. The SSRL Structural Molecular Biology Program is supported by the Department of Energy, Office of Biological and Environmental Research, and by the National Institutes of Health, National Center for Research Resources, Biomedical Technology Program, and the National Institute of General Medical Sciences. We thank members of the Purification groups within Genentech Small Molecule Drug Discovery for analytical support and thank also the Genentech Oligonucleotide and DNA Sequencing groups.

Supporting Information Available: Preliminary SAR from focused combinatorial libraries, kinase selectivity panel for inhibitors **13** and **9**, data collection and refinement statistics for crystal structures, and NMR spectra for compounds **5** and **9**−**14**. This material is available free of charge via the Internet at http://pubs.acs.org.

References

(1) Carmena, M.; Earnshaw, W. C. The cellular geography of Aurora kinases. *Nat. Rev. Mol. Cell Biol.* **2003**, *4*, 842–854.
(2) Marumoto, T.; Zhang, D.; Saya, H. Aurora-A, a guardian of poles. *Nat. Rev. Cancer* **2005**, *5*, 42–50.
(3) Keen, N.; Taylor, S. Aurora-kinase inhibitors as anticancer agents. *Nat. Rev. Cancer* **2004**, *4*, 927–936.
(4) Andrews, P. D. Aurora kinases: shining lights on the therapeutic

horizon. *Oncogene* **2005**, *24*, 5005–5015.
(5) Jackson, J. R.; Patrick, D. R.; Dar, M. M.; Huang, P. S. Targeted anti-mitotic therapies: can we improve on tubulin agents? *Nat. Rev. Cancer* **2007**, *7*, 107–117.
(6) Giet, R.; Petretti, C.; Prigent, C. Aurora kinases, aneuploidy and cancer, a coincidence or a real link. *Trends Cell Biol.* **2005**, *15*, 241–250.
(7) Ditchfield, C.; Johnson, V. L.; Tighe, A.; Ellston, R.; Haworth, C.; Johnson, T.; Mortlock, A.; Keen, N.; Taylor, S. S. Aurora B couples chromosome alignment with anaphase by targeting BubR1, Mad2, and Cenp-E to kinetochores. *J. Cell Biol.* **2003**, *161*, 267–280.
(8) Hauf, S.; Cole, R. W.; LaTerra, S.; Zimmer, C.; Schnapp, G.; Walter, R.; Heckel, A.; van Meel, J.; Rieder, C.; Peters, J. M. The small molecule Hesperadin reveals a role for Aurora B in correcting kinetochore-microtubule attachment and in maintaining the spindle assembly checkpoint. *J. Cell Biol.* **2003**, *161*, 281–294.
(9) Harrington, E. A.; Bebbington, D.; Moore, J.; Rasmussen, R. K.; Ajose-Adeogun, A. O.; Nakayama, T.; Graham, J. A.; Demmur, C.; Hercend, T.; Diu-Hercend, A.; Su, M.; Golec, J. M. C.; Miller, K. M. VX-680, a potent and selective small-molecule inhibitor of the Aurora kinases, suppresses tumor growth in vivo. *Nat. Med.* **2004**, *10*, 262–267.
(10) Wilkinson, R. W.; Odedra, R.; Heaton, S. P.; Wedge, S. R.; Keen, N. J.; Crafter, C.; Foster, J. R.; Brady, M. C.; Bigley, A.; Brown, E.; Byth, K. F.; Barrass, N. C.; Mundt, K. E.; Foote, K. M.; Heron, N. M.; Jung, F. H.; Mortlock, A. A.; Boyle, F. T.; Green, S. AZD1152, a selective inhibitor of Aurora B kinase, inhibits human tumor xenograft growth by inducing apoptosis. *Clin. Cancer Res.* **2007**, *13*, 3682–3688.
(11) Girdler, F.; Sessa, F.; Patercoli, S.; Villa, F.; Musacchio, A.; Taylor, S. Molecular basis of drug resistance in Aurora kinases. *Chem. Biol.* **2008**, *15*, 552–562.
(12) Bischoff, J. R.; Anderson, L.; Zhu, Y.; Mossie, K.; Ng, L.; Souza, B.; Schryver, B.; Flanagan, P.; Clairvoyant, F.; Ginther, C.; Chan, C. S. M.; Novotny, M.; Slamon, D. J.; Plowman, G. D. A homologue of *Drosophila aurora* kinase is oncogenic and amplified in human colorectal cancers. *EMBO J.* **1998**, *17*, 3052–3065.
(13) Zhou, H.; Kuang, J.; Zhong, L.; Kuo, W.; Gray, J. W.; Sahin, A.; Brinkley, B. R.; Sen, S. Tumour amplified kinase STK15/BTAK induces centrosome amplification, aneuploidy and transformation. *Nat. Genet.* **1998**, *20*, 189–193.
(14) Anand, S.; Penrhyn-Lowe, S.; Venkitaraman, A. R. AURORA-A amplification overrides the mitotic spindle checkpoint, inducing resistance to Taxol. *Cancer Cell* **2003**, *3*, 51–62.
(15) Meraldi, P.; Honda, R.; Nigg, E. A. Aurora kinases link chromosome segregation and cell division to cancer susceptibility. *Curr. Opin. Genet. Dev.* **2004**, *14*, 29–36.
(16) Sen, S.; Zhou, H.; White, R. A. A putative serine/threonine kinase encoding gene BTAK on chromosome 20q13 is amplified and overexpressed in human breast cancer cell lines. *Oncogene* **1997**, *14*, 2195–2200.
(17) Manfredi, M. G.; Escedy, J. A.; Meetze, K. A.; Balani, S. K.; Burenkova, O.; Chen, W.; Galvin, K. M.; Hoar, K. M.; Huck, J. J.; LeRoy, P. J.; Ray, E. T.; Sells, T. B.; Stringer, B.; Stroud, S. G.; Vos, T. J.; Weatherhead, G. S.; Wysong, D. R.; Zhang, M.; Bolen, J. B.; Claiborne, C. F. Antitumor activity of MLN8054, an orally active small-molecule inhibitor of Aurora A kinase. *Proc. Natl. Acad. Sci. U.S.A.* **2007**, *104*, 4106–4111.
(18) Masuda, A.; Maeno, K.; Nakagawa, T.; Saito, H.; Takahashi, T. Association between mitotic spindle checkpoint impairment and susceptibility to the induction of apoptosis by anti-microtubule agents in human lung cancers. *Am. J. Pathol.* **2003**, *163*, 1109–1116.
(19) Sudo, T.; Nitta, M.; Saya, H.; Ueno, N. T. Dependence of paclitaxel sensitivity on a functional spindle assembly checkpoint. *Cancer Res.* **2004**, *64*, 2502–2508.
(20) Weaver, B. A. A.; Cleveland, D. W. Decoding the links between mitosis, cancer, and chemotherapy: the mitotic checkpoint, adaptation, and death. *Cancer Cell* **2005**, *8*, 7–12.
(21) Nitta, M.; Kobayashi, O.; Honda, S.; Hirota, T.; Kuninaka, S.; Marumoto, T.; Ushio, Y.; Saya, H. Spindle checkpoint function is required for mitotic catastrophe induced by DNA-damaging agents. *Oncogene* **2004**, *23*, 6548–6558.
(22) Jiang, Y.; Zhang, Y.; Lees, E.; Seghezzi, W. Aurora A overexpression overrides the mitotic spindle checkpoint triggered by nocodozole, a microtubule destabilizer. *Oncogene* **2003**, *22*, 8293–8301.
(23) Hata, T.; Furukawa, T.; Sunamura, M.; Egawa, S.; Motoi, F.; Ohmura, N.; Marumoto, T.; Saya, H.; Horii, A. RNA interference targeting Aurora kinase A suppresses tumor growth and enhances the taxane chemosensitivity in human pancreatic cancer cells. *Cancer Res.* **2005**, *65*, 2899–2905.
(24) Breault, G. A.; Ellston, R. P. A.; Green, S.; James, S. R.; Jewsbury, P. J.; Midgley, C. J.; Pauptit, R. A.; Minshull, C. A.; Tucker, J. A.; Pease, J. E. Cyclin-dependent kinase 4 inhibitors as a treatment for cancer. Part 2: Identification and optimisation of substituted 2,4-bis anilino pyrimidines. *Bioorg. Med. Chem. Lett.* **2003**, *13*, 2961–2966.
(25) Beattie, J. F.; Breault, G. A.; Ellston, R. P. A.; Green, S.; Jewsbury, P. J.; Midgley, C. J.; Naven, R. T.; Minshull, C. A.; Pauptit, R. A.; Tucker, J. A.; Pease, J. E. Cyclin-dependent kinase 4 inhibitors as a treatment for cancer. Part 1: Identification and optimisation of substituted 4,6-bis anilino pyrimidines. *Bioorg. Med. Chem. Lett.* **2003**, *13*, 2955–2960.
(26) Anderson, M.; Beattie, J. F.; Breault, G. A.; Breed, J.; Byth, K. F.; Culshaw, J. D.; Ellston, R. P. A.; Green, S.; Minshull, C. A.; Norman, R. A.; Pauptit, R. A.; Stanway, J.; Thomas, A. P.; Jewsbury, P. J. Imidazo[1,2-*a*]pyridines: a potent and selective class of cyclin-dependent kinase inhibitors identified through structure-based hybridisation. *Bioorg. Med. Chem. Lett.* **2003**, *13*, 3021–3026.
(27) Tari, L. W.; Hoffman, I. D.; Bensen, D. C.; Hunter, M. J.; Nix, J.; Nelson, K. J.; McRee, D. J.; Swanson, R. V. Structural basis of the inhibition of Aurora A kinase by a novel class of high-affinity disubstituted pyrimidine inhibitors. *Bioorg. Med. Chem. Lett.* **2007**, *17*, 688–691.
(28) Zhang, Q.; Liu, Y.; Gao, F.; Ding, Q.; Cho, C.; Hur, W.; Jin, Y.; Uno, T.; Joazeiro, C. A. P.; Gray, N. Discovery of EGFR selective 4,6-disubstituted pyrimidines from a combinatorial kinase-directed heterocycle library. *J. Am. Chem. Soc.* **2006**, *128*, 2182–2183.
(29) Moriarty, K. J.; Koblish, H. K.; Garrabrant, T.; Maisuria, J.; Khalil, E.; Ali, F.; Petrounia, I. P.; Crysler, C. S.; Maroney, A. C.; Johnson, D. L.; Galemmo, R. A., Jr. The synthesis and SAR of 2-amino-pyrrolo[2,3-*d*]pyrimidines: a new class of Aurora-A kinase inhibitors. *Bioorg. Med. Chem. Lett.* **2006**, *16*, 5778–5783.
(30) Rawson, T. E.; Rüth, M.; Blackwood, E.; Burdick, D.; Corson, L.; Dotson, J.; Drummond, J.; Fields, C.; Georges, G. J.; Goller, B.; Halladay, J.; Hunsaker, T.; Kleinheinz, T.; Krell, H.-W.; Li, J.; Liang, J.; Limberg, A.; McNutt, A.; Moffat, J.; Phillips, G.; Ran, Y.; Safina, B.; Ultsch, M.; Walker, L.; Wiesmann, C.; Zhang, B.; Zhou, A.; Zhu, B.-Y.; Rüger, P.; Cochran, A. G. A pentacyclic Aurora kinase inhibitor (AKI-001) with high in vivo potency and oral bioavailability. *J. Med. Chem.* **2008**, *51*, 4465–4475.
(31) Bayliss, R.; Sardon, T.; Vernos, I.; Conti, E. Structural basis of Aurora-A activation by TPX2 at the mitotic spindle. *Mol. Cell* **2003**, *12*, 851–862.
(32) Cochran, A. G. Aurora A: target invalidated? *Chem. Biol.* **2008**, *15*, 525−526.
(33) Tao, W.; South, V. J.; Zhang, Y.; Davide, J. P.; Farrell, L.; Kohl, N. E.; Sepp-Lorenzino, L.; Lobell, R. B. Induction of apoptosis by an inhibitor of the mitotic kinesin KSP requires both activation of the spindle assembly checkpoint and mitotic slippage. *Cancer Cell* **2005**, *8*, 49–59.
(34) Gascoigne, K. E.; Taylor, S. S. Cancer cells display profound intra- and inter-line variation following prolonged exposure to antimitotic drugs. *Cancer Cell* **2008**, *14*, 1–12.
(35) Delano, W. L. *The PyMOL Molecular Graphics System*; DeLano Scientific: Palo Alto, CA, 2002.
(36) Nowakowski, J.; Cronin, C. N.; McRee, D. E.; Knuth, M. W.; Nelson, C.; Pavletich, N. P.; Rodgers, J.; Sang, B.-C.; Scheibe, D. N.; Swanson, R. V.; Thompson, D. A. Structures of the cancer-related Aurora-A, FAK and EphA2 protein kinases from nanovolume crystallography. *Structure* **2002**, *10*, 1659–1667.
(37) Myrianthopoulos, V.; Magiatis, P.; Ferandin, Y.; Skaltsounis, A.-L.; Meijer, L.; Mikros, E. An integrated computational approach to the phenomenon of potent and selective inhibition of Aurora kinases B and C by a series of 7-substituted indirubins. *J. Med. Chem.* **2007**, *50*, 4027–4037.
(38) Buzko, O.; Shokat, K. M. A kinase sequence database: sequence alignments and family assignment. *Bioinformatics* **2002**, *18*, 1274–1275.
(39) Knighton, D. R.; Zheng, J.; Ten Eyck, L. F.; Xuong, N.; Taylor, S. S.; Sowadski, J. M. Structure of a peptide bound to the catalytic subunit of cyclic adenosine monophosphate-dependent protein kinase. *Science* **1991**, *253*, 414–420.

JM9000314